

Free-electron-laser near-field nanospectroscopy

Cite as: Appl. Phys. Lett. **73**, 151 (1998); <https://doi.org/10.1063/1.121739>

Submitted: 15 January 1998 . Accepted: 08 May 1998 . Published Online: 07 July 1998

A. Cricenti, R. Generosi, P. Perfetti, J. M. Gilligan, N. H. Tolk, C. Coluzza, and G. Margaritondo



View Online



Export Citation

ARTICLES YOU MAY BE INTERESTED IN

Near-field optical microscopy with an infra-red free electron laser applied to cancer diagnosis
Applied Physics Letters **102**, 053701 (2013); <https://doi.org/10.1063/1.4790436>

Scanning near-field optical microscopy with aperture probes: Fundamentals and applications
The Journal of Chemical Physics **112**, 7761 (2000); <https://doi.org/10.1063/1.481382>

Optical stethoscopy: Image recording with resolution $\lambda/20$
Applied Physics Letters **44**, 651 (1984); <https://doi.org/10.1063/1.94865>



Free-electron-laser near-field nanospectroscopy

A. Cricenti, R. Generosi, and P. Perfetti

Istituto di Struttura della Materia, CNR, via Fosso del Cavaliere, 00133 Roma, Italy

J. M. Gilligan and N. H. Tolk

Department of Physics and Astronomy, Vanderbilt University, Nashville, Tennessee 37235

C. Coluzza

Dipartimento di Fisica, Università di Roma "La Sapienza," P.le A. Moro 2, 00185 Roma, Italy

G. Margaritondo^{a)}

Institut de physique appliquée, Ecole Polytechnique Fédérale, CH-1015 Lausanne, Switzerland

(Received 15 January 1998; accepted for publication 8 May 1998)

First experiments at the Vanderbilt free electron lasers measured the local reflectivity of a PtSi/Si system. The reflectivity in the scanning near-field optical microscope images revealed features that were not present in the corresponding shear-force (topology) images and which were due to localized changes in the bulk properties of the sample. The size of the smallest detected features clearly demonstrated that near-field conditions were reached. The use of different photon wavelengths (0.653, 1.2, and 2.4 μm) enabled us to probe regions of different depth. © 1998 American Institute of Physics. [S0003-6951(98)01128-0]

We demonstrated that free-electron-laser (FEL) spectroscopy can be implemented in scanning near-field optical microscopy (SNOM) conditions, thereby providing an excellent probe to study space variations of important materials properties. The successful tests were performed detecting the reflected infrared radiation of the Vanderbilt FEL with a SNOM. We specifically succeeded in measuring the local bulk optical properties of the PtSi/Si system with lateral resolution well below the diffraction limit.

Infrared spectroscopy with a FEL is an excellent probe of semiconductor interfaces whose energy barriers and discontinuities fall in this spectral domain.^{1,2} Contrary to conventional electron spectroscopy approaches, the FEL radiation has a deep penetration and can analyze technologically realistic buried interfaces.² These investigations, however, are affected by a severe limitation common to many other interface studies: lack of lateral resolution. Many interface properties and phenomena, in fact, change significantly from place to place.^{3,4} The lack of lateral resolution may lead to misleading or incomplete results, and makes it impossible to really understand many microelectronic devices.

This limitation can be removed by using a SNOM apparatus in which a stretched optical fiber with a very small open edge aperture collects the reflected radiation—thereby reaching resolution levels beyond the diffraction limit. The SNOM technique importance is growing rapidly in characterizing materials with spatial resolution far below the classical diffraction limit.^{5–7} This can nondestructively study localized variations in buried interfaces.⁸

The local FEL-SNOM reflectivity measurements were complemented by shear-force measurements⁵⁻⁷ revealing the corresponding local surface topology. This enabled us to distinguish topological features from true lateral variations of the optical properties of the sample.

Figure 1 shows the experimental setup. The Vanderbilt FEL electron beam is produced by a 45-meV-radiofrequency accelerator, operating at a frequency up to 2.856 GHz. The emitted infrared radiation is continuously tunable over the 2–10 μm wavelength (extended to 1 μm by second-harmonic generation) with high output power and brightness. Pulses with 6 ms duration, 360 mJ energy, and 11 W average power (repetition rate 30 Hz) were reliably demonstrated for 4.8 mm wavelength.

Our SNOM⁹ is a two-piece cylinder, similar to the atomic-force microscope (AFM) we described in Ref. 10. The detection system is on the upper part and the sample scanning devices in the lower part. The piezoelectric scanning range is $17 \times 17 \times 5 \text{ } \mu\text{m}^3$. The tip-sample distance is controlled by a shear-force feedback system⁵ and the topographic vertical resolution is 1 nm. The tip of the optical fiber was stretched obtaining a few tens of nanometer wide pinhole.

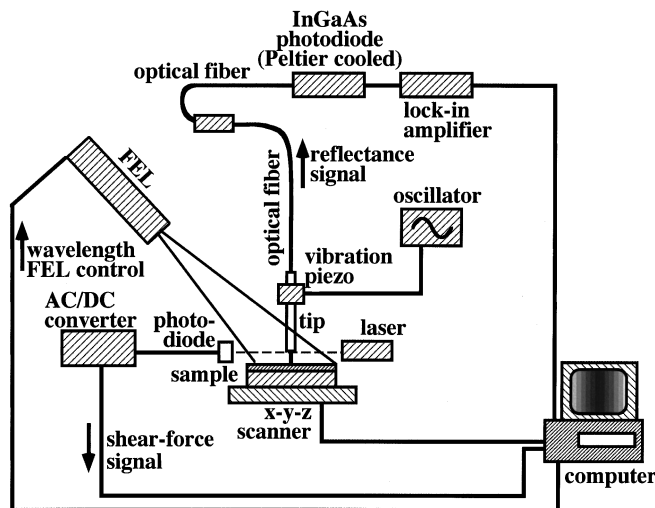


FIG. 1. Scheme of the experimental setup.

^{a)}Electronic mail: marga@dpmail.epfl.ch

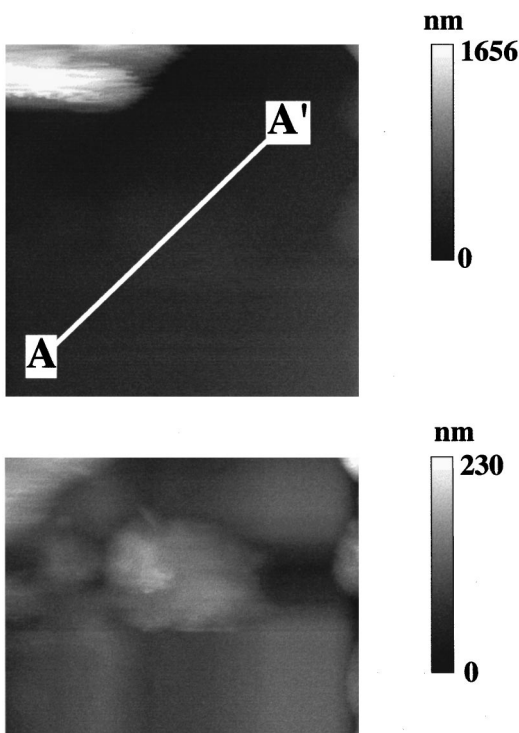


FIG. 2. (a) $12 \times 12 \mu\text{m}^2$ shear-force topography image; (b) shear-force image taken from the lower part of the previous figure.

Infrared reflectivity images were obtained by detecting the reflected intensity while scanning the fiber position relative to the sample. We used two different FEL wavelengths: 1.2 and $2.4 \mu\text{m}$. In addition, we also performed experiments with a 5 mW He–Ne laser ($0.63 \mu\text{m}$ wavelength). The reflectivity was measured with a standard loc-in technique. Topographic images were obtained by measuring the shear-force signal with a synchronous detection including a piezoelectric oscillator and an alternating current/direct current (ac/dc) converter.¹¹

Successful tests were performed studying a PtSi/Si system, obtained by evaporating 4 nm of Pt on a Si substrate (previous cleaned with standard techniques) at room temperature. The sample was then annealed at 350°C to form the interface.

Figure 2(a) is a $12 \times 12 \mu\text{m}^2$ shear force image. Brighter areas correspond to higher topography values (or to higher reflectivity in the optical images shown later). No filtering

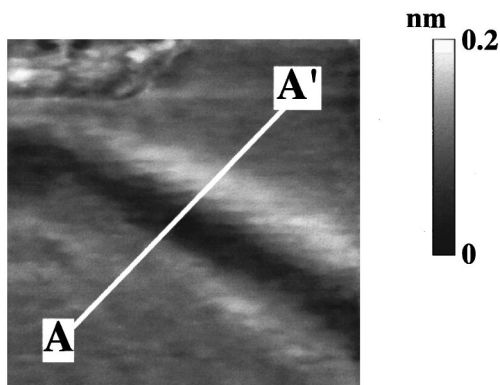


FIG. 3. Reflectivity image corresponding to Fig. 2(b), taken with a photon wavelength of $2.4 \mu\text{m}$.

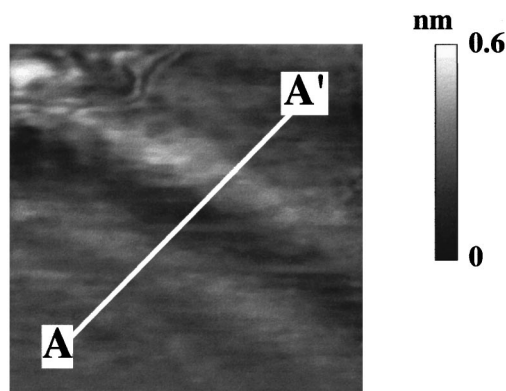


FIG. 4. Reflectivity image corresponding to Fig. 2(b), taken with a photon wavelength of $1.2 \mu\text{m}$.

was performed except for a background and plane alignment.

A rather big structure (corrugation 1500 nm) is visible in the upper left corner. This is an anomalous feature: the shear-force images are, in general, quite smooth with corrugation not exceeding a few tens of nanometers. However, the strongly corrugated area was also visible in the optical images; thus, we used it to correlate the two types of images. Figure 2(b) shows the portion of Fig. 2(a) below the strongly corrugated area with a different dynamic range, revealing weaker topographic contrast and, in particular, a round structure with 150 nm corrugation.

Figure 3 is a reflectivity image of the same area of Fig. 2(a) for $2.4 \mu\text{m}$ wavelength. The strongly corrugated feature is still visible, but in addition we see a 1000 nm wide, 0.2 mV deep transversal “valley.” Note that the valley is not at all correlated to topographic structure at the center of Fig. 2(b). Furthermore, due to the deep penetration of the infrared light its origin must be well below the surface; we tentatively attribute it to a Si groove. The corrugation on the surface does not appear to influence in this case the reflectivity contrast.

Figure 4 is a reflectivity image similar to Fig. 3 for $1.2 \mu\text{m}$ wavelength. The transverse valley of purely optical origin is still clearly visible. This is no longer true for the image of Fig. 5, taken at $0.63 \mu\text{m}$ wavelength; whereas, the strongly corrugated upper-left-corner structure is still visible.

Figure 6 shows the line contours taken along the marked lines of Figs. 2(b), 3, 4, and 5. The topographic line (a) reveals a corrugation 150 nm. Lines b (Fig. 3) and c (Fig. 4)

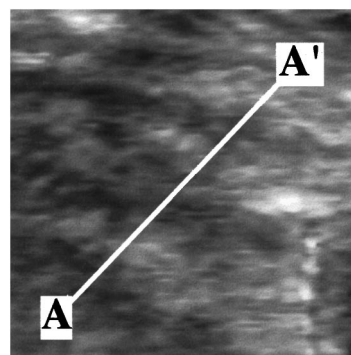


FIG. 5. Reflectivity image corresponding to Fig. 2(b), taken with a photon wavelength of $0.63 \mu\text{m}$.

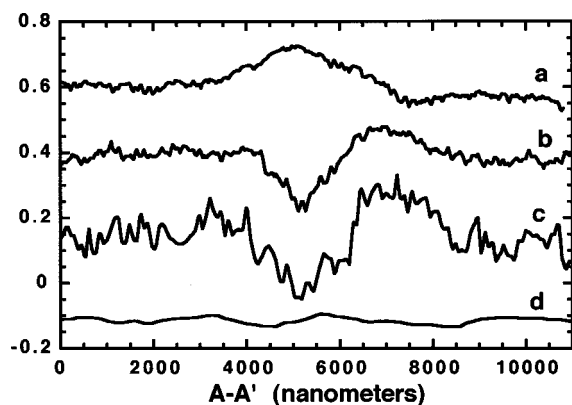


FIG. 6. Profiles along the marked lines in (a) The topography Fig. 2(b) (mm); (b)–(d) the optical reflectivity Figs. 3–5.

show the reflectivity minimum of the valley. Line d (Fig. 5) shows no reflectivity variations within the experimental uncertainty. This indicates that the valley in the 2.4 and 1.2 μm images is deeper than the maximum penetration of 0.63 μm photons at our incidence angle of 75° from the normal direction.

The valley observed in Figs. 3 and 4 could be due to the silicon-silicide interface. This possibility is being tested by extending the same approach to other infrared spectroscopy modes, thanks to the flexibility of our multipurpose SNOM module.⁹ We already obtained some photocurrent images by illuminating the sample through the optical fiber. A similar approach can be used to detect very small lateral variations of interface barrier heights.⁸

An upper limit for the lateral resolution was estimated from the edge slope of the smallest detected features in a large number of images. We conclude that the resolution was better than 100 nm for topographic images, and than 200–400 nm for reflectivity images. Although these values, in the best case better than $\lambda/10$, are most likely underestimates,

they are already well below the $\lambda/2$ level—demonstrating that the main objective of near-field conditions was achieved.

First tests of this novel FEL-SNOM combination are quite encouraging. No major problems were encountered, a new-field condition was clearly achieved, and the technique appears feasible to a huge variety of buried interface studies. The combination of reflection and shear-force measurements provides a clear distinction between topographic variations at the surface and variations in optical properties. This correlation test is not possible with other optical microscopic techniques and makes the FEL-SNOM combination uniquely useful for studying buried interfaces. Future work will provide a clear picture of lateral variations in interface properties and of their influence on the behavior and performance of microelectronic devices.

The authors are grateful to the entire staff of the Vanderbilt FEL for their expert technical support. Work was supported by the Italian National Research Council, the U.S. Office of Naval Research, the Fonds National de la Recherche Scientifique, and the Ecole Polytechnique Fédérale de Lausanne.

¹E. Yuncel *et al.*, Phys. Rev. Lett. **70**, 4146 (1993).

²C. Coluzza *et al.*, Phys. Rev. B **46**, 12834 (1992).

³C. Coluzza *et al.*, J. Appl. Phys. **76**, 3710 (1994).

⁴G. Margaritondo, F. Gozzo, and C. Coluzza, Phys. Rev. B **47**, 9907 (1993).

⁵E. Betzig, P. L. Finn, and J. S. Wiener, Appl. Phys. Lett. **60**, 2484 (1994).

⁶NATO ASI Series, *Near Field Optics*, edited by D. W. Pohl and D. Courjon (Kluwer Academic, Dordrecht, 1992), Vol. 262.

⁷J. Almeida *et al.*, Appl. Phys. Lett. **69**, 2361 (1996).

⁸C. Coluzza, J. Almeida, T. dell'Orto, O. Bergossi, M. Spajer, S. Davy, D. Courjon, A. Cricenti, R. Generosi, P. Perfetti, and G. Faini, Proc. SPIE **2782**, 591 (1997).

⁹A. Cricenti, R. Generosi, C. Barchesi, M. Luce, and M. Rinaldi (unpublished).

¹⁰A. Cricenti and R. Generosi, Rev. Sci. Instrum. **66**, 2843 (1995).

¹¹C. Barchesi, A. Cricenti, R. Generosi, C. Giammichele, M. Luce, and M. Rinaldi, Rev. Sci. Instrum. **68**, 3799 (1997).